



# HHS Public Access

Author manuscript

*Genesis*. Author manuscript; available in PMC 2023 September 27.

Published in final edited form as:

*Genesis*. 2023 September ; 61(5): e23516. doi:10.1002/dvg.23516.

## Characterizing expression pattern of *Six2Cre* during mouse craniofacial development

Meenakshi Umar,

Chunmin Dong,

Fenglei He

Department of Cell and Molecular Biology, School of Science and Engineering, Tulane University, New Orleans, Louisiana, USA

### Summary

Craniofacial development is a complex process involving diverse cell populations. Various transgenic Cre lines have been developed to facilitate studying gene function in specific tissues. In this study, we have characterized the expression pattern of *Six2Cre* mice at multiple stages during craniofacial development. Our data revealed that *Six2Cre* lineage cells are predominantly present in frontal bone, mandible, and secondary palate. Using immunostaining method, we found that *Six2Cre* triggered reporter is co-expressed with *Runx2*. In summary, our data showed *Six2Cre* can be used to study gene function during palate development and osteogenesis in mouse models.

### Keywords

craniofacial development; lineage tracing; mouse; osteogenesis; palate

## 1 | INTRODUCTION

Craniofacial development is an intricate process involving diverse cell populations. These cells are mainly derived from two origins: neural crest and mesoderm. Neural crest cells give rise to majority of bone, cartilage, and connective tissues in facial skeleton (Chai et al., 2000; Jiang, Rowitch, Soriano, McMahon, & Sucov, 2000; McBratney-Owen,

This is an open access article under the terms of the [Creative Commons Attribution-NonCommercial-NoDerivs License](#), which permits use and distribution in any medium, provided the original work is properly cited, the use is non-commercial and no modifications or adaptations are made.

**Correspondence:** Fenglei He, Department of Cell and Molecular Biology, School of Science and Engineering, Tulane University, New Orleans, LA, USA. [fhe@tulane.edu](mailto:fhe@tulane.edu).

#### AUTHOR CONTRIBUTIONS

Fenglei He: conceptualization, methodology and manuscript writing. Meenakshi Umar: methodology, manuscript writing, experiment and data analysis. Chunmin Dong: experiment and data analysis. All authors contributed to review and approved the submission.

#### CONFLICT OF INTEREST STATEMENT

The authors declare no conflicts of interest.

#### ETHICS STATEMENT

All animal experiments were conducted according to protocol approved by the Institutional Animal Care and Use Committee of Tulane University.

#### SUPPORTING INFORMATION

Additional supporting information can be found online in the Supporting Information section at the end of this article.

Iseki, Bamforth, Olsen, & Morriss-Kay, 2008; Yoshida, Vivatbutisiri, Morriss-Kay, Saga, & Iseki, 2008). The mesoderm mainly contributes to muscle but also to bone, cartilage, and connective tissues in cranial base and calvarium (Gage, Rhoades, Prucka, & Hjalt, 2005; McBratney-Owen et al., 2008; Trainor & Tam, 1995; Yoshida et al., 2008). Genetic engineering technique using Cre and loxP provides a valuable tool to study role of genes in specific tissues. Multiple Cre lines have been generated for this purpose. Of these, *Wnt1Cre* (Danielian, Muccino, Rowitch, Michael, & McMahon, 1998), *Wnt1Cre2* (Lewis, Vasudevan, O'Neill, Soriano, & Bush, 2013), *POCre* (Yamauchi et al., 1999), *Sox10Cre* (Matsuoka et al., 2005), and *Mef2c-F10NCre* (Aoto et al., 2015) are used to analyze neural crest cells. *Mesp1Cre* (Saga et al., 1999) and *Prx1Cre* (Logan et al., 2002) target mesoderm derived cells. However, since both neural crest and mesoderm give rise to a wide range of tissues and these Cre lines are expressed early in development, optimized Cre tools are needed to study gene function in specific tissues.

*Six2* encodes a transcription factor with restricted expression pattern in developing embryos (He et al., 2010; Liu et al., 2019; Ohto et al., 1998; Okello et al., 2017; Oliver et al., 1995). *Six2Cre* transgenic mouse line was first generated to study nephron progenitor cells, but *Six2Cre* lineage cells are also found in post-migratory neural crest derivatives (Kobayashi et al., 2008), suggesting it a potential tool to study tissue-specific function of genes in craniofacial development. We thus employed *R26R<sup>tdT</sup>* reporter mice in combination with *Six2Cre* to assess the spatiotemporal expression of this transgene in the head (Madisen et al., 2010). Our data revealed that *Six2Cre* lineage cells are detected in the secondary palate, frontal bone, and mandible. In the bony tissues, we confirmed co-localization of *Six2Cre* triggered reporter with Runx2, suggesting that *Six2Cre* mice can be used to study osteogenesis in a tissue-specific manner.

## 2 | MATERIALS AND METHODS

### 2.1 | Mice

All animal studies were in compliance with the protocol approved by the Institutional Animal Care and Use Committee of Tulane University. The following mice strains were used in the study: *Tg(Six2-EGFP/cre)<sup>IAmc/J</sup>* (Kobayashi et al., 2008) (JAX stock #009606), referred to as *Six2Cre*, was maintained on *C57BL/6 J;129SvJaeSor* mixed genetic background; and *Gt(ROSA)26.Sor<sup>tm9(CAG-tdTomato)Hze</sup>* (Madisen et al., 2010), referred to as *R26R<sup>tdT</sup>*, was maintained on *C57BL/6J* background. For embryo collection, vaginal plug was checked daily, and the midday when vaginal plug was observed was considered as embryonic day (E) 0.5. For postnatal animals, the day on which pups were born was counted as postnatal day 0 (P0).

### 2.2 | Histology

Timed embryos and postnatal pups were collected at designated day. The head samples were dissected in ice-cold phosphate buffer saline (PBS) and fixed in 4% paraformaldehyde (PFA)/PBS overnight at 4°C. Samples were then dehydrated in gradient sucrose/PBS washes and embedded in OCT. Frozen samples were sectioned in 8 µm. Alkaline phosphatase-Alcian blue (AP-AB) staining was performed as described previously (Dong et al., 2019). In

short, sections were incubated with 0.03% nitro-blue tetrazolium chloride (NBT) (Roche, 11383213001) and 0.02% 5-bromo-4-chloro-3-indolylphosphate *p*-toluidine salt (BCIP) (Roche, 11383221001) in NTMT solution (100 mM NaCl, 100 mM Tris pH 9.5, 50 mM MgCl<sub>2</sub> and 0.1% Tween-20 in distilled water). When AP signal was fully developed, slides were rinsed with distilled water then were immersed in 1% alcian blue 8GX (Sigma, A5268) in 0.1 N HCl, and then counterstained with 0.1% nuclear fast red (Acros Organics, 211980050) in 0.08 M aluminum sulfate (Al<sub>2</sub>(SO<sub>4</sub>)<sub>3</sub>·18H<sub>2</sub>O).

### 2.3 | Wholemount fluorescent imaging

Staged embryos and postnatal pups were dissected in ice-cold PBS. *Six2Cre;R26R<sup>tdT</sup>* mice heads were imaged from lateral, dorsal and ventral sides with or without mandible using Nikon SMZ18 stereomicroscope.

### 2.4 | Immunofluorescence staining

The immunofluorescence staining was performed using standard protocol as described previously (Bartoletti, Dong, Umar, & He, 2020). Briefly, slides were blocked with 5% donkey serum for 1 hr and then incubated in primary antibody solution overnight at 4°C. Following washes in PBS with 0.1% Tween-20, sections were incubated with secondary antibody for 1 hr at room temperature. Sections were later mounted with VECTASHIELD antifade mounting media with DAPI (Vector laboratories, H-1200). Following primary and secondary antibodies were used in the study: anti-Runx2 (Cell Signaling Technology, 12556, 1:200), anti-Six2 (Proteintech, 11562-1-AP, 1:200) and Alexa fluor-488 (Thermo Fisher Scientific, A21206, 1:400).

## 3. | RESULTS

To trace *Six2Cre* lineage cells in craniofacial tissues, we have generated *Six2Cre;R26R<sup>tdT</sup>* mice and examined the expression pattern of tdTomato reporter at multiple stages. Wholemount examination of E13.5 *Six2Cre;R26R<sup>tdT</sup>* embryonic head shows the presence of tdTomato+ cells in regions around supra orbital arch (soa), mandible (md), maxilla (mx), pinna, pituitary gland, and palatal shelf (ps) (Figure 1a–d). Similar expression pattern of tdTomato was observed in E16.5 and P0 samples (Figure 1e–l).

To identify detailed expression pattern of *Six2Cre*, we have examined tdTomato expression in coronal sections of *Six2Cre;R26R<sup>tdT</sup>* at both anterior and posterior level. At anterior level, tdTomato expression is observed in cartilage of nasal septum (ns), olfactory epithelium (oe), ps, mx, and md (Figure 2a). AP-AB staining at same level reveals location of ns chondrocytes and osteoblasts (Figure 2b). Similar expression pattern between tdTomato and staining confirms *Six2Cre* lineage cells in ns chondrocytes and osteoblasts in maxilla and distal mandibular mesenchyme (Figure 2a,b). At posterior level, tdTomato expression is observed in region around frontal bone (fb), ps, and md (Figure 2c). AP-AB staining shows the pattern of chondrocytes and osteoblasts (Figure 2d) at the same level as indicated in Figure 2e. We have further compared expression pattern of tdTomato and endogenous Six2. At E13.5, tdTomato expression in *Six2Cre;R26R<sup>tdT</sup>* is mostly overlapped with endogenous Six2 protein in ns cartilage, oe, fb, ala orbitalis (ao), md, and ps (Figure S1a–c).

At E16.5, *Six2Cre* triggered tdTomato expression exhibits a pattern resembling that in E13.5 embryo. At anterior level, *Six2Cre* lineage cells are detected in oe, ns cartilage, premaxilla (pmx), mx, md, and the tongue mesenchyme (Figure 3a,a'). AP-AB staining at same level revealed location of chondrocytes of ns and osteoblasts (Figure 3b,b'), in a pattern overlapped with tdTomato (Figure 3a,a',b,b'). At posterior level, tdTomato expression is detected in fb, ao, ps, and md, in a pattern overlapped with AP or AB staining signal (Figure 3c,d). Section levels of E16.5 head in Figure 3a–d are indicated in Figure 3e. Similar to tdTomato reporter expression, endogenous *Six2* expression is observed in ns cartilage, oe, fb, ao, mx, ps, and md in *Six2Cre* lineage cells (Figure S2a–d).

At P0, tdTomato expression is still detected in oe, ns cartilage, and mx at anterior level (Figure 4a,b). At posterior level, tdTomato expression is found in the fb and AP-positive cells next to ao (Figure 4c,d). It is also detected in the fused palatal shelf in a pattern overlapped with AP signals around molars and md (Figure 4e,f). The section levels of P0 head in Figure 4a–f are indicated in Figure 4g. Endogenous *Six2* expression is observed in ns cartilage, oe, fb, mx, ps and md in *Six2Cre* descendants at P0 (Figure S3a–d).

The overlapped expression pattern of tdTomato with AP signal (Figures 2, 3, and 4) suggests that many *Six2Cre* descendants are osteoblasts. To test this hypothesis, we have examined *Runx2* expression in *Six2Cre;R26R<sup>tdT</sup>* using immunostaining method. Our data show that at E16.5, tdTomato expression is overlapped with *Runx2* in fb (Figure 5a,c,d). In upper molar, *Runx2* expression is weak in dental epithelium (de) and strong in surrounding dental mesenchyme (dm), mx and ps (Figure 5e,g). Extensive overlapping of *Runx2* with tdTomato is detected in dm, mx, and ps (Figure 5e,g,h). Similar expression pattern is also detected in the lower molar. *Runx2* exhibits overlapped expression pattern with tdTomato in the dm and md (Figure 5i,k,l).

We have further examined *Runx2* expression pattern in *Six2Cre;R26R<sup>tdT</sup>* mice at P0. Similar to that in E16.5, *Runx2* expression is overlapped with tdTomato in fb (Figure 6a,c,d). *Runx2* is barely detected in ameloblast (am) in upper and lower molar and strongly expressed in ps, mx, and md (Figure 6e,g,i,k). *Runx2* expression remains overlapped with tdTomato in mx, ps, and md (Figure 6e,g–i,k,l). These results are in line with our observation in E16.5 embryos, and support the notion that *SixCre* descendants are predominant in preosteoblasts.

## 4 | DISCUSSION

Genetic engineering technique using Cre-loxP provides valuable tool to study genes' function in specific tissues, which is usually impeded by early embryonic lethality of null mutant. Generation and identification of tissue-specific Cre lines thus are critical in these studies. Here, we traced *Six2Cre* lineage in developing embryos, with a focus on craniofacial tissues. Previous report showed that *Six2Cre* triggered reporter is expressed in post-migratory neural crest cells in craniofacial mesenchyme after E10.5 (Kobayashi et al., 2008). In this study, our data revealed that *Six2Cre* descendants predominantly contribute to the secondary palate, mandible and frontal bone. In addition, we identified that *Six2Cre* triggered reporter is co-expressed with *Runx2*, suggesting that *Six2Cre* can

be used to analyze gene function in palate mesenchyme and osteoblasts during craniofacial development.

Several Cre lines have been utilized in studies of palate development. Of these, *Nestin-Cre* shows activity in epithelium and mesenchyme of palate (Liu et al., 2005). *K14Cre* and *Pitx2Cre* have been used to examine gene function in palate epithelium (He et al., 2010; Xiong et al., 2009). *Osr2Cre* is expressed in the palate mesenchyme (He, Popkie, et al., 2010; Lan, Wang, Ovitt, & Jiang, 2007; Song et al., 2013). However, a subset of *Osr2Cre* mice exhibits ubiquitous expression pattern (Lan et al., 2007). Compared to *Osr2Cre*, *Six2Cre* mice exhibit restricted expression pattern in palate mesenchyme consistently, and does not have such a caveat. In addition, our study revealed that *Six2Cre* triggered reporter is co-expressed with Runx2 in palate at E16.5 and P0 (Figures 5 and 6). Taken together, these results suggest *Six2Cre* is a useful tool to study gene function in palate mesenchyme.

Calvarial bones are formed through intramembranous ossification, in which mesenchymal cells differentiate directly into osteoblasts (Hall & Miyake, 2000). Previous study reported that *Six2Cre* lineage cells contribute to osteoblast and osteocytes in frontal bones (Farmer et al., 2021). In line to this, we observed *Six2Cre* lineage cells expressed Runx2 in frontal bone, palate and mandible (Figures 5 and 6). These results suggest that *Six2Cre* descendants contribute to calvarial osteoblasts.

Mouse tooth development is a multi-step process marked by distinct gene expression. Previous studies have shown that at E12–E16, dental mesenchymal cells, ameloblasts and odontoblasts show strong Runx2 expression (Chen et al., 2009; Yamashiro, Aberg, Levanon, Groner, & Thesleff, 2002). At E18 and postnatal stages, Runx2 expression is barely detected in dental pulp cells, ameloblasts and odontoblasts (Chen et al., 2009; Yamashiro et al., 2002). In present study, we also observed strong expression of Runx2 in dental mesenchyme cells but no expression in ameloblasts (Figures 5 and 6). In line with previous reports, our findings support that Runx2 is involved in distinct stages of tooth development, and that *Six2Cre* can be used to study gene function in dental mesenchyme in a tissue-specific manner.

*Six2* is expressed in cranial base, and plays an important role in its development (He, Tavella, et al., 2010; Liu et al., 2019). We thus examined tdTomato reporter expression in cranial base of *Six2Cre;R26R<sup>tdT</sup>* embryo. Surprisingly, sagittal sections of E16.5 *Six2Cre;R26R<sup>tdT</sup>* head and AP-AB staining in parallel sections fail to identify tdTomato+ cells in cranial base cartilages (Figure S4a,b). These data show that *Six2Cre* lineage cells do not contribute to cranial base cartilages. Since *Six2Cre* is a BAC transgenic allele, the discrepancy in expression between endogenous *Six2* mRNA and *Six2Cre* could reflect the general technical limitation of transgenes.

## Supplementary Material

Refer to Web version on PubMed Central for supplementary material.

## ACKNOWLEDGMENTS

The authors are grateful to the He laboratory members for the comments. *Six2Cre* line is obtained from Drs. Samir El-Dahr and Hongbing Liu. This work was supported by Tulane University and NIH/National Institute of Dental and Craniofacial Research grant DE028918 to F.H.

### Funding information

NIH/National Institute of Dental and Craniofacial Research; Tulane University

## DATA AVAILABILITY STATEMENT

The data that support the findings of this study are available from the corresponding author upon reasonable request.

## REFERENCES

- Aoto K, Sandell LL, Butler Tjaden NE, Yuen KC, Watt KE, Black BL, ... Trainor PA (2015). Mef2c-F10N enhancer driven beta-galactosidase (LacZ) and Cre recombinase mice facilitate analyses of gene function and lineage fate in neural crest cells. *Developmental Biology*, 402(1), 3–16. 10.1016/j.ydbio.2015.02.022 [PubMed: 25794678]
- Bartoletti G, Dong C, Umar M, & He F (2020). Pdgfra regulates multipotent cell differentiation towards chondrocytes via inhibiting Wnt9a/beta-catenin pathway during chondrocranial cartilage development. *Developmental Biology*, 466(1–2), 36–46. 10.1016/j.ydbio.2020.08.004 [PubMed: 32800757]
- Chai Y, Jiang X, Ito Y, Bringas P Jr., Han J, Rowitch DH, ... Sucov HM (2000). Fate of the mammalian cranial neural crest during tooth and mandibular morphogenesis. *Development*, 127(8), 1671–1679. 10.1242/dev.127.8.1671 [PubMed: 10725243]
- Chen S, Gluhak-Heinrich J, Wang YH, Wu YM, Chuang HH, Chen L, ... MacDougall M (2009). Runx2, osx, and dspp in tooth development. *Journal of Dental Research*, 88(10), 904–909. 10.1177/0022034509342873 [PubMed: 19783797]
- Danielian PS, Muccino D, Rowitch DH, Michael SK, & McMahon AP (1998). Modification of gene activity in mouse embryos in utero by a tamoxifen-inducible form of Cre recombinase. *Current Biology*, 8(24), 1323–1326. 10.1016/s0960-9822(07)00562-3 [PubMed: 9843687]
- Dong C, Umar M, Bartoletti G, Gahankari A, Fidelak L, & He F (2019). Expression pattern of Kmt2d in murine craniofacial tissues. *Gene Expression Patterns*, 34, 119060. 10.1016/j.gep.2019.119060 [PubMed: 31228576]
- Farmer DT, Mlcochova H, Zhou Y, Koelling N, Wang G, Ashley N, ... Twigg SRF (2021). The developing mouse coronal suture at single-cell resolution. *Nature Communications*, 12(1), 4797. 10.1038/s41467-021-24917-9
- Gage PJ, Rhoades W, Prucka SK, & Hjalt T (2005). Fate maps of neural crest and mesoderm in the mammalian eye. *Investigative Ophthalmology & Visual Science*, 46(11), 4200–4208. 10.1167/iovs.05-0691 [PubMed: 16249499]
- Hall BK, & Miyake T (2000). All for one and one for all: Condensations and the initiation of skeletal development. *BioEssays*, 22(2), 138–147. 10.1002/(SICI)1521-1878(200002)22:2<138::AID-BIES5>3.0.CO;2-4 [PubMed: 10655033]
- He F, Popkie AP, Xiong W, Li L, Wang Y, Phiel CJ, & Chen Y (2010). Gsk3beta is required in the epithelium for palatal elevation in mice. *Developmental Dynamics*, 239(12), 3235–3246. 10.1002/dvdy.22466 [PubMed: 20981831]
- He G, Tavella S, Hanley KP, Self M, Oliver G, Grifone R, – Bobola N (2010). Inactivation of Six2 in mouse identifies a novel genetic mechanism controlling development and growth of the cranial base. *Developmental Biology*, 344(2), 720–730. 10.1016/j.ydbio.2010.05.509 [PubMed: 20515681]
- Jiang X, Rowitch DH, Soriano P, McMahon AP, & Sucov HM (2000). Fate of the mammalian cardiac neural crest. *Development*, 127(8), 1607–1616. 10.1242/dev.127.8.1607 [PubMed: 10725237]

- Kobayashi A, Valerius MT, Mugford JW, Carroll TJ, Self M, Oliver G, & McMahon AP (2008). Six2 defines and regulates a multipotent self-renewing nephron progenitor population throughout mammalian kidney development. *Cell Stem Cell*, 3(2), 169–181. 10.1016/j.stem.2008.05.020 [PubMed: 18682239]
- Lan Y, Wang Q, Ovitt CE, & Jiang R (2007). A unique mouse strain expressing Cre recombinase for tissue-specific analysis of gene function in palate and kidney development. *Genesis*, 45(10), 618–624. 10.1002/dvg.20334 [PubMed: 17941042]
- Lewis AE, Vasudevan HN, O'Neill AK, Soriano P, & Bush JO (2013). The widely used Wnt1-Cre transgene causes developmental phenotypes by ectopic activation of Wnt signaling. *Developmental Biology*, 379(2), 229–234. 10.1016/j.ydbio.2013.04.026 [PubMed: 23648512]
- Liu W, Sun X, Braut A, Mishina Y, Behringer RR, Mina M, & Martin JF (2005). Distinct functions for Bmp signaling in lip and palate fusion in mice. *Development*, 132(6), 1453–1461. 10.1242/dev.01676 [PubMed: 15716346]
- Liu Z, Li C, Xu J, Lan Y, Liu H, Li X, ... Jiang R (2019). Crucial and overlapping roles of Six1 and Six2 in craniofacial development. *Journal of Dental Research*, 98(5), 572–579. 10.1177/0022034519835204 [PubMed: 30905259]
- Logan M, Martin JF, Nagy A, Lobe C, Olson EN, & Tabin CJ (2002). Expression of Cre recombinase in the developing mouse limb bud driven by a Prx1 enhancer. *Genesis*, 33(2), 77–80. 10.1002/gene.10092 [PubMed: 12112875]
- Madisen L, Zwingman TA, Sunkin SM, Oh SW, Zariwala HA, Gu H, ... Zeng H (2010). A robust and high-throughput Cre reporting and characterization system for the whole mouse brain. *Nature Neuroscience*, 13(1), 133–140. 10.1038/nn.2467 [PubMed: 20023653]
- Matsuoka T, Ahlberg PE, Kessar N, Iannarelli P, Dennehy U, Richardson WD, ... Koentges G (2005). Neural crest origins of the neck and shoulder. *Nature*, 436(7049), 347–355. 10.1038/nature03837 [PubMed: 16034409]
- McBratney-Owen B, Iseki S, Bamforth SD, Olsen BR, & Morriss-Kay GM (2008). Development and tissue origins of the mammalian cranial base. *Developmental Biology*, 322(1), 121–132. 10.1016/j.ydbio.2008.07.016 [PubMed: 18680740]
- Ohto H, Takizawa T, Saito T, Kobayashi M, Ikeda K, & Kawakami K (1998). Tissue and developmental distribution of six family gene products. *The International Journal of Developmental Biology*, 42(2), 141–148. [PubMed: 9551859]
- Okello DO, Iyyanar PPR, Kulyk WM, Smith TM, Lozanoff S, Ji S, & Nazarali AJ (2017). Six2 plays an intrinsic role in regulating proliferation of mesenchymal cells in the developing palate. *Frontiers in Physiology*, 8, 955. 10.3389/fphys.2017.00955 [PubMed: 29218017]
- Oliver G, Mailhos A, Wehr R, Copeland NG, Jenkins NA, & Gruss P (1995). Six3, a murine homologue of the sine oculis gene, demarcates the most anterior border of the developing neural plate and is expressed during eye development. *Development*, 121(12), 4045–4055. 10.1242/dev.121.12.4045 [PubMed: 8575305]
- Saga Y, Miyagawa-Tomita S, Takagi A, Kitajima S, Miyazaki J, & Inoue T (1999). MesP1 is expressed in the heart precursor cells and required for the formation of a single heart tube. *Development*, 126(15), 3437–3447. 10.1242/dev.126.15.3437 [PubMed: 10393122]
- Song Z, Liu C, Iwata J, Gu S, Suzuki A, Sun C, ... Chen Y (2013). Mice with Tak1 deficiency in neural crest lineage exhibit cleft palate associated with abnormal tongue development. *The Journal of Biological Chemistry*, 288(15), 10440–10450. 10.1074/jbc.M112.432286 [PubMed: 23460641]
- Trainor PA, & Tam PP (1995). Cranial paraxial mesoderm and neural crest cells of the mouse embryo: co-distribution in the craniofacial mesenchyme but distinct segregation in branchial arches. *Development*, 121(8), 2569–2582. 10.1242/dev.121.8.2569 [PubMed: 7671820]
- Xiong W, He F, Morikawa Y, Yu X, Zhang Z, Lan Y, ... Chen Y (2009). Hand2 is required in the epithelium for palatogenesis in mice. *Developmental Biology*, 330(1), 131–141. 10.1016/j.ydbio.2009.03.021 [PubMed: 19341725]
- Yamashiro T, Aberg T, Levanon D, Groner Y, & Thesleff I (2002). Expression of Runx1, -2 and -3 during tooth, palate and craniofacial bone development. *Mechanisms of Development*, 119(Suppl 1), S107–S110. 10.1016/s0925-4773(03)00101-1 [PubMed: 14516670]

- Yamauchi Y, Abe K, Mantani A, Hitoshi Y, Suzuki M, Osuzu F, ... Yamamura K (1999). A novel transgenic technique that allows specific marking of the neural crest cell lineage in mice. *Developmental Biology*, 212(1), 191–203. 10.1006/dbio.1999.9323 [PubMed: 10419695]
- Yoshida T, Vivatbutsiri P, Morriss-Kay G, Saga Y, & Iseki S (2008). Cell lineage in mammalian craniofacial mesenchyme. *Mechanisms of Development*, 125(9–10), 797–808. 10.1016/j.mod.2008.06.007 [PubMed: 18617001]

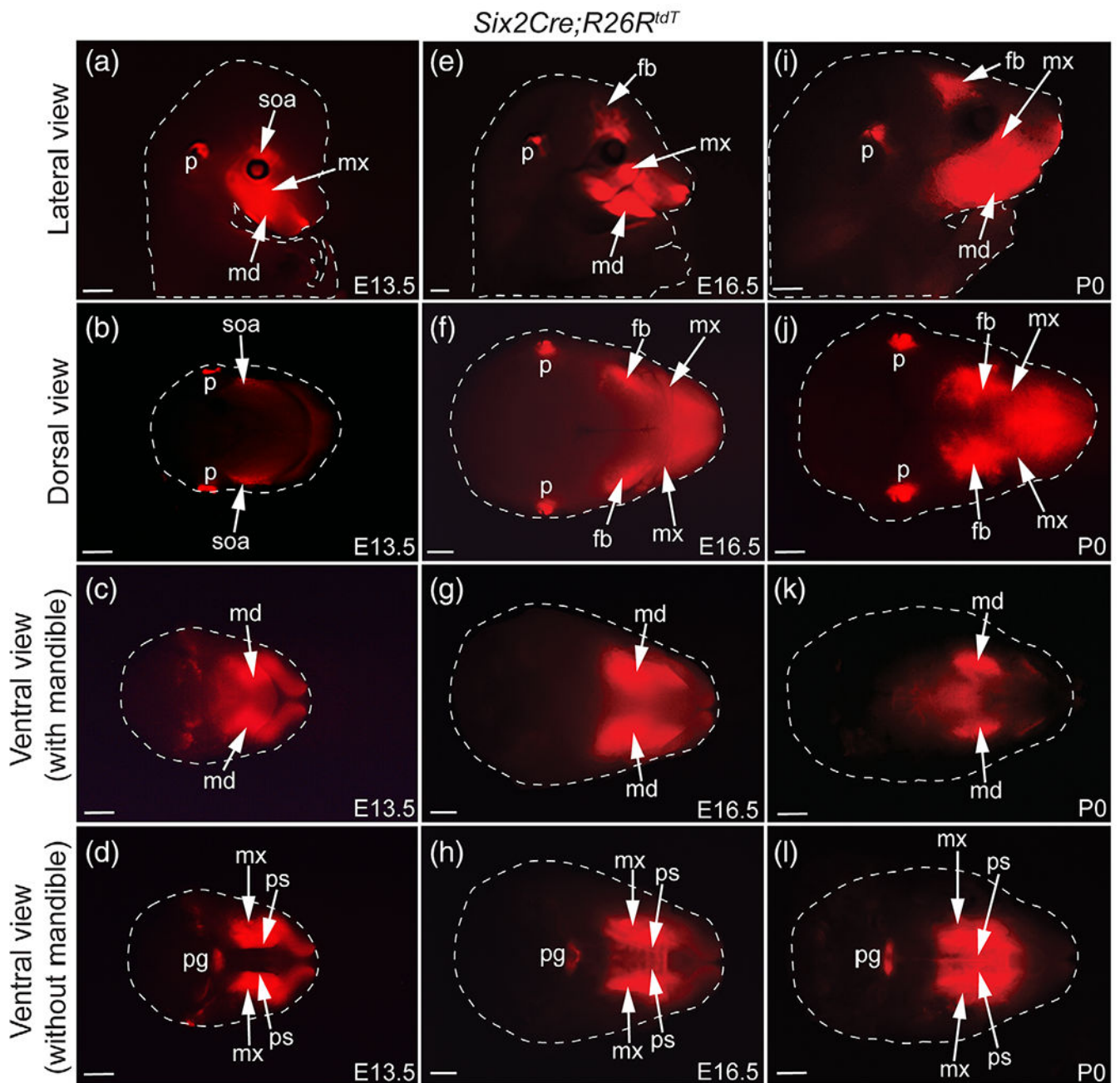
Author Manuscript

Author Manuscript

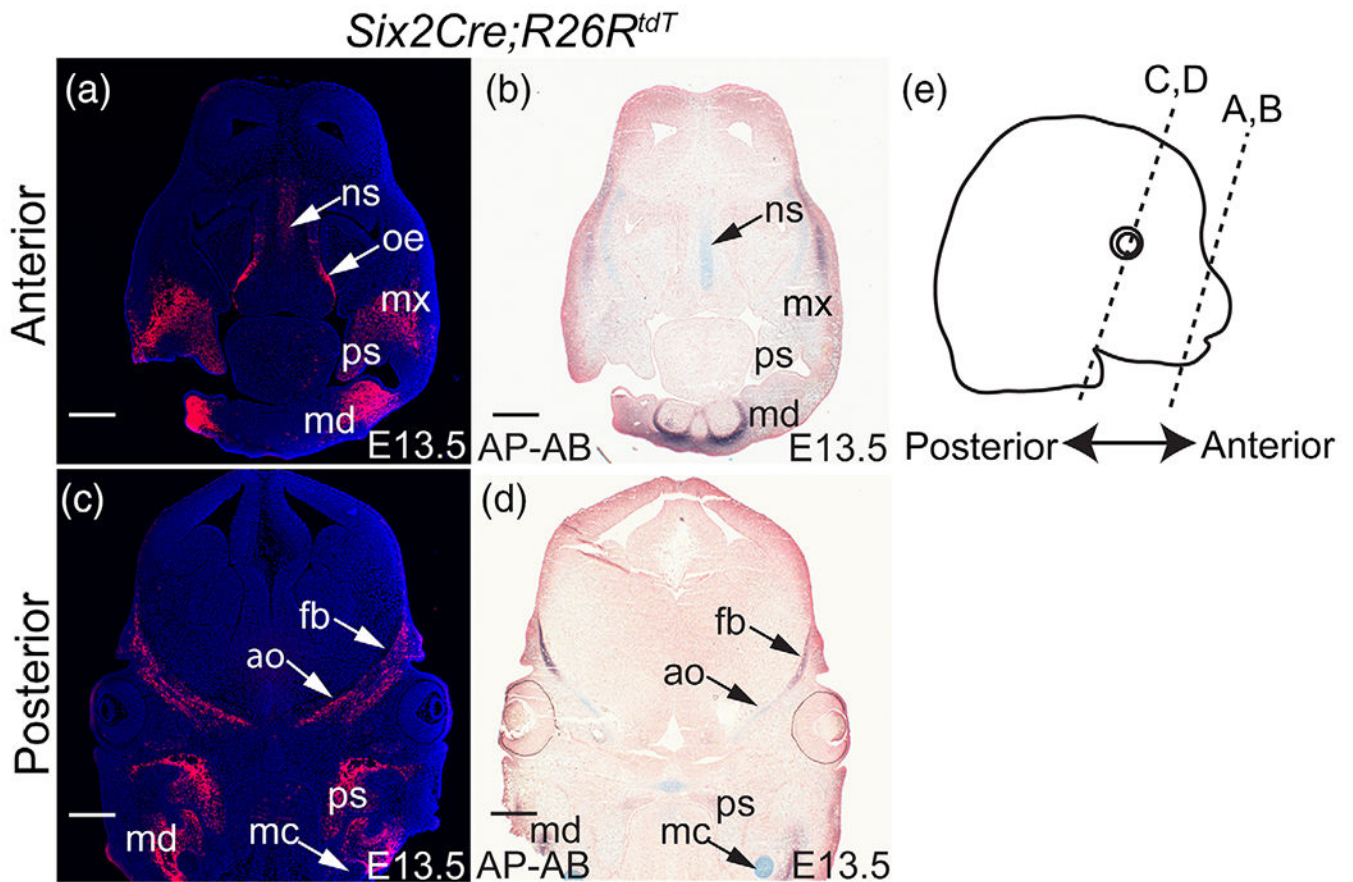
Author Manuscript

Author Manuscript



**FIGURE 1.**

Wholemount views of *Six2Cre;R26R<sup>tdT</sup>* head at (a–d) E13.5, (e–h) E16.5 and at (i–l) P0. Embryonic (E13.5 and E16.5) and P0 heads of *Six2Cre;R26R<sup>tdT</sup>* were imaged at different angles to show lateral views (a, e, i), dorsal views (b, f, j), ventral views with mandible (c, g, k) and without mandible (d, h, l). fb, frontal bone; md, mandible; mx, maxilla; p, pinna; pg, pituitary gland; ps, palatal shelf; soa, supraorbital arch. Scale bar, 1 mm.

**FIGURE 2.**

Expression pattern of tdTomato reporter in *Six2Cre;R26R<sup>tdT</sup>* head at E13.5. (a, b) Coronal sections of E13.5 *Six2Cre;R26R<sup>tdT</sup>* head at anterior level show (a) tdTomato reporter expression and DAPI staining and (b) AP-AB staining. (c, d) Coronal sections of E13.5 *Six2Cre;R26R<sup>tdT</sup>* head at posterior level show (c) tdTomato reporter expression and DAPI staining and (d) AP-AB staining. (e) Illustration of E13.5 head shows section levels in A-D. ao, ala orbitalis; fb, frontal bone; mc, Meckel's cartilage; md, mandible; mx: maxilla; ns, nasal septum; oe, olfactory epithelium; ps, palatal shelf. Scale bar, 500  $\mu$ m.

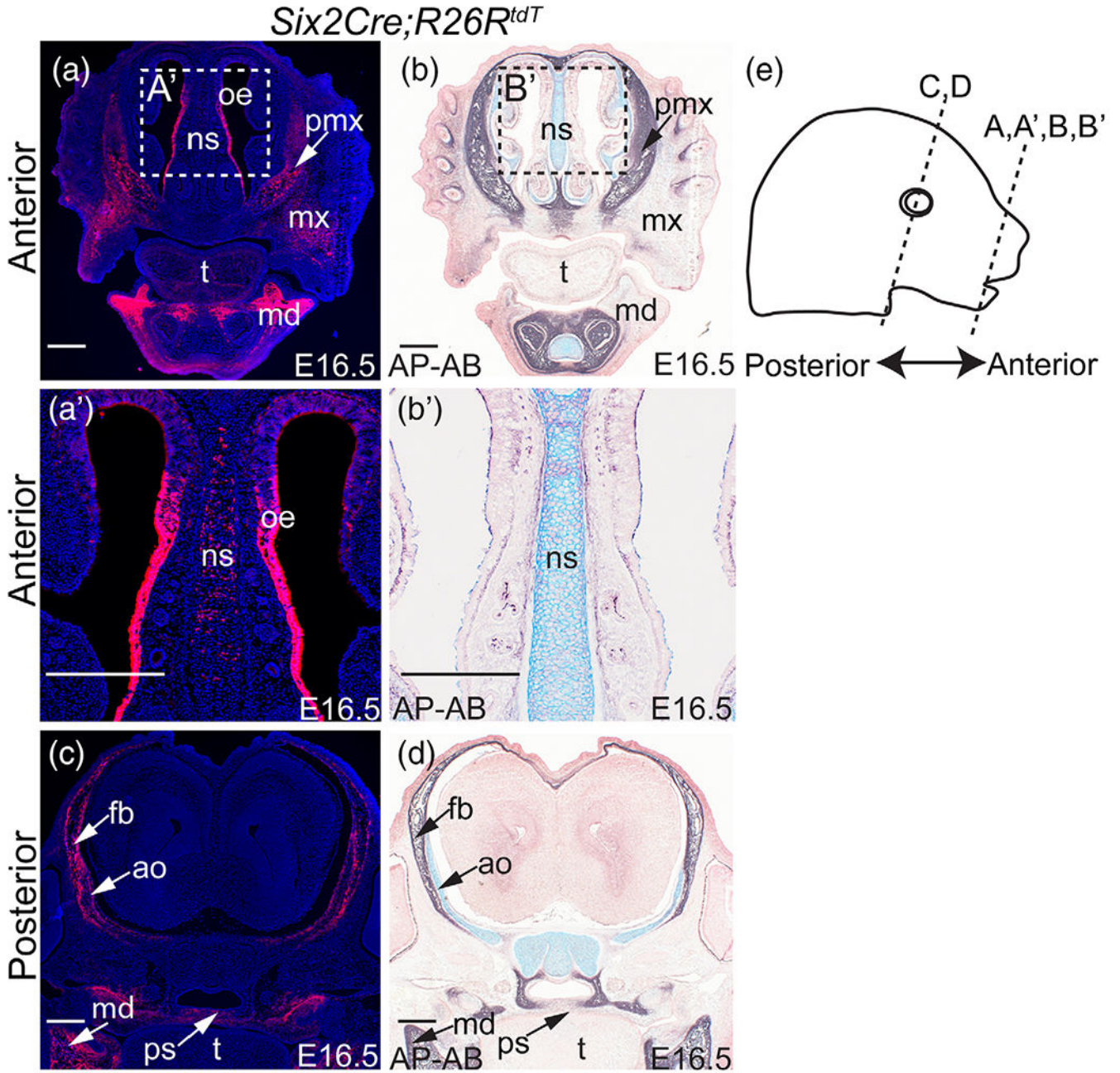


**FIGURE 3.** Expression pattern of tdTomato reporter in *Six2Cre;R26R<sup>tdT</sup>* head at E16.5. (a, a') tdTomato expression on coronal section of E16.5 *Six2Cre;R26R<sup>tdT</sup>* head at anterior level. Sections were counterstained with DAPI. (a') is inset of (a). (b, b') AP-AB staining on coronal section at the same level. (b') is inset of (b). (c) tdTomato expression on coronal section of E16.5 *Six2Cre;R26R<sup>tdT</sup>* head at posterior level. Sections were counterstained with DAPI. (d) AP-AB staining on coronal section at the comparable level to (c). (e) Illustration of E16.5 head shows section levels in (a–d). ao, ala orbitalis; fb, frontal bone; md, mandible; mx,

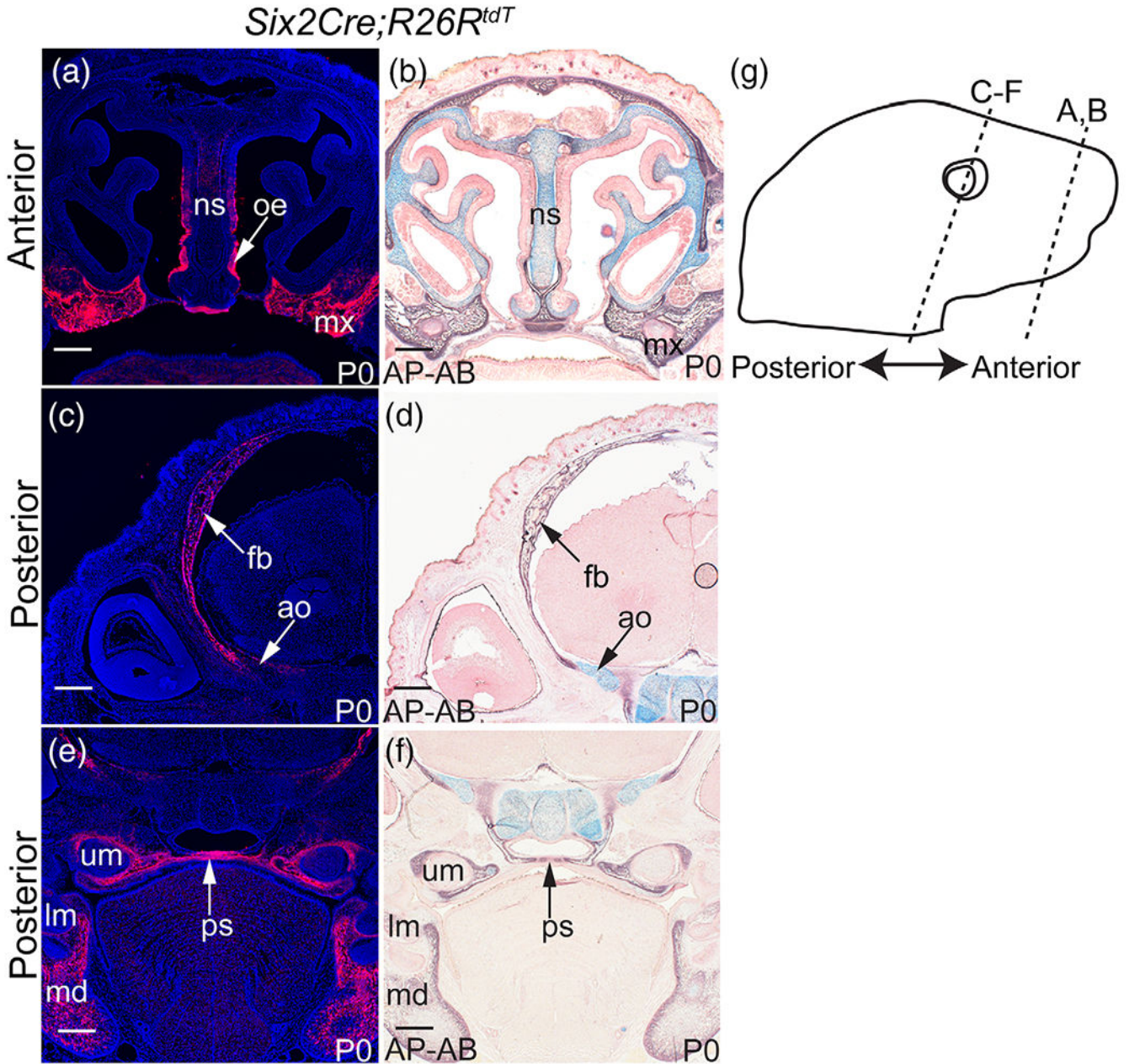
maxilla; ns, nasal septum; oe, olfactory epithelium; pmx, premaxilla; ps, palatal shelf; t, tongue. Scale bar, 500  $\mu\text{m}$ .

Author Manuscript

Author Manuscript

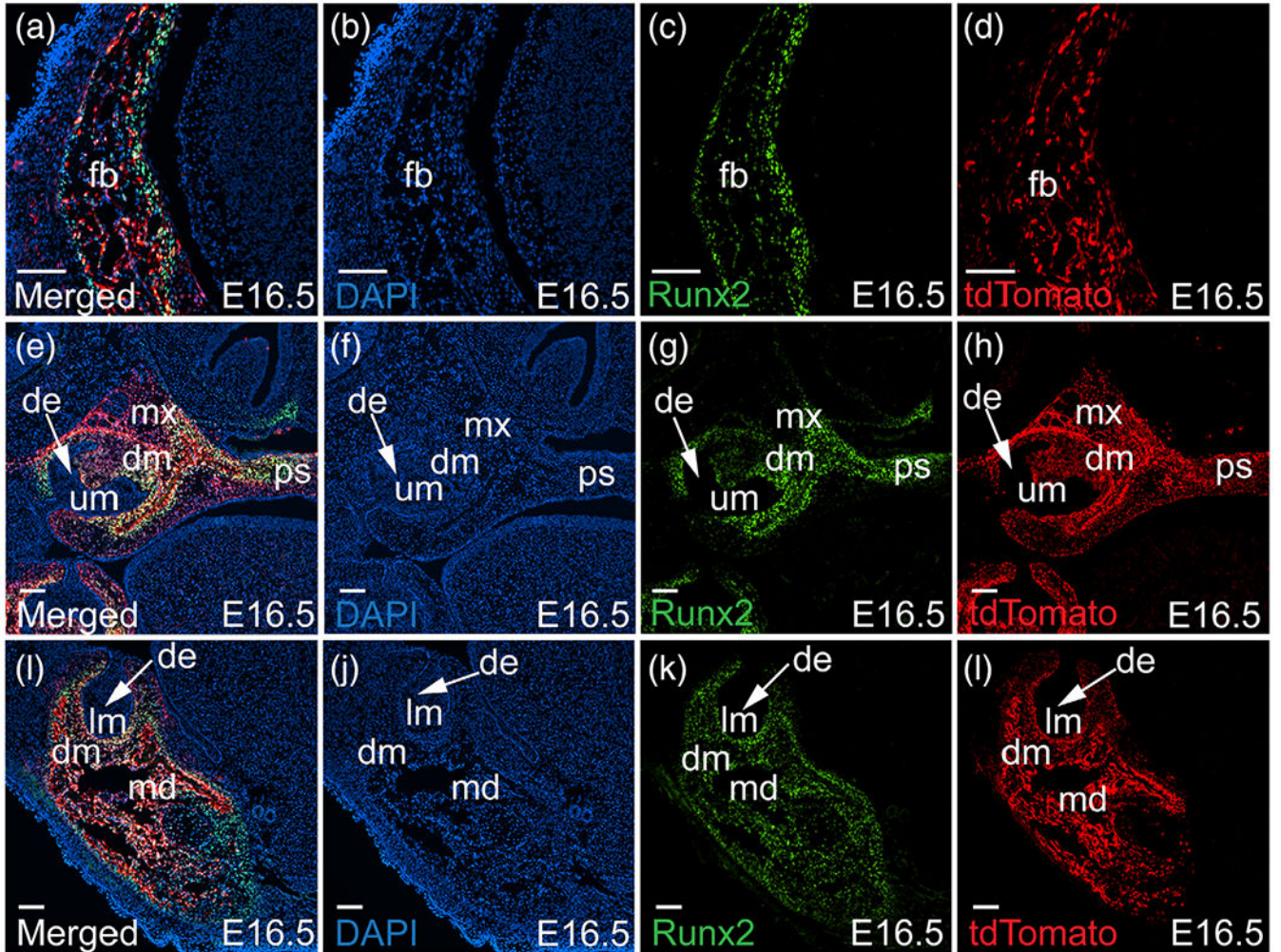
Author Manuscript

Author Manuscript

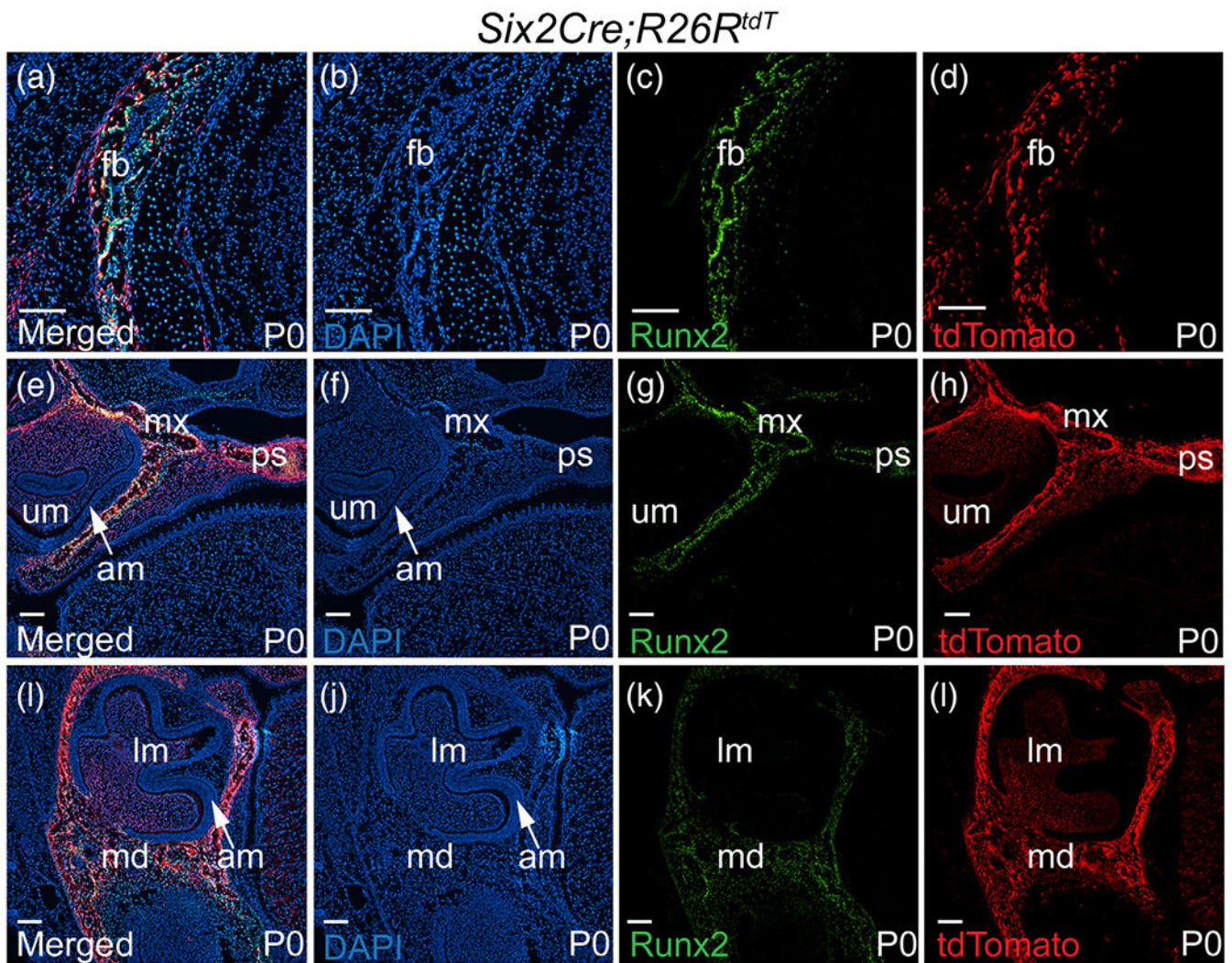


**FIGURE 4.**

Expression pattern of tdTomato reporter in *Six2Cre;R26R<sup>tdT</sup>* head at P0. (a, b) Coronal sections of P0 *Six2Cre;R26R<sup>tdT</sup>* head at anterior level show (a) tdTomato expression and DAPI staining and (b) AP-AB staining. (c–f) Coronal sections of P0 *Six2Cre;R26R<sup>tdT</sup>* head at posterior level show (c,e) tdTomato expression and DAPI staining and (d, f) AP-AB staining. (g) Illustration of P0 head shows section levels in (a–f). ao, ala orbitalis; fb, frontal bone; lm, lower molar; md, mandible; mx, maxilla; ns, nasal septum; oe, olfactory epithelium; ps, palatal shelf; um, upper molar. Scale bar, 500  $\mu$ m.

*Six2Cre;R26R<sup>tdT</sup>***FIGURE 5.**

Co-expression of tdTomato reporter and Runx2 in coronal sections of *Six2Cre;R26R<sup>tdT</sup>* head at E16.5. (a–l) Immunofluorescence staining on coronal sections of E16.5 *Six2Cre;R26R<sup>tdT</sup>* head show tdTomato expression (d, h, l) with anti-Runx2 antibody (c, g, k). Sections were counterstained with DAPI (b, f, j) and merged images are shown in (a, e, and i). de, dental epithelium; dm, dental mesenchyme; fb, frontal bone; lm, lower molar; md, mandible; mx, maxilla, ps, palatal shelf; um, upper molar. Scale bar, 100  $\mu$ m.

**FIGURE 6.**

Co-localization of tdTomato reporter and Runx2 in *Six2Cre;R26R<sup>tdT</sup>* at P0. (a–l) Immunofluorescence staining on coronal sections of P0 *Six2Cre;R26R<sup>tdT</sup>* head show tdTomato expression (d, h, l) with anti-Runx2 antibody (c, g, k). Sections were counterstained with DAPI (b, f, j) and merged images are shown in (a, e, and i). am, ameloblast; fb, frontal bone; lm, lower molar; md, mandible; mx, maxilla; ps, palatal shelf; um, upper molar. Scale bar, 100  $\mu$ m.